

## Analysis of Three and Five-phase Double Stator Slotted Rotor Permanent Magnet Generator (DSSR-PMG)

R. Suhairi<sup>1</sup>, R. N. Firdaus<sup>2</sup>, F. Azhar<sup>3</sup>, K. A. Karim<sup>4</sup>, A. Jidin<sup>5</sup>, A. Khamis<sup>6</sup>, Z. Ibrahim<sup>7</sup>, T. Sutikno<sup>8</sup>

<sup>1,2,3,4,5,6,7</sup> Faculty of Electrical Engineering, Universiti Teknikal Malaysia Melaka (UTeM), Malaysia

<sup>1,2,3,4,5,6,7</sup> Electrical Machine Design, Power Electronics and Drives Research Group, CeRIA, UTeM, Malaysia

<sup>1</sup> Electrical Technology Section, Universiti Kuala Lumpur-British Malaysian Institute, Malaysia

<sup>8</sup> Department of Electrical Engineering, Universitas Ahmad Dahlan, Indonesia

---

### Article Info

#### Article history:

Received Oct 08, 2016

Revised Dec 14, 2016

Accepted Dec 24, 2016

---

#### Keyword:

Double stator

Permanent magnet

Slotted rotor

---

### ABSTRACT

This paper discusses the performance of three and five-phase double stator slotted rotor permanent magnet generator (DSSR-PMG). The objective of this research is to propose five-phase DSSR-PMG structure that could minimize output voltage ripple compared to three phase. In this research Finite Element Analysis (FEA) is used to simulate the characteristic of the three and five-phase permanent magnet generator at various speeds. The characteristic of back-EMF, flux linkage, cogging torque and flux density for three and five-phase configurations is presented. As a result, five-phase DSSR-PMG shows a lower cogging torque and voltage ripple compared to three-phase. The cogging torque for five-phase is 80% lower than three-phase DSSR-PMG and the ripple voltage (peak to peak) of back-EMF in five-phase is 2.3% compared to the three-phase DSSR-PMG which is 55%.

Copyright © 2017 Institute of Advanced Engineering and Science.  
All rights reserved.

---

### Corresponding Author:

R. N. Firdaus,  
Faculty of Electrical Engineering,  
Universiti Teknikal Malaysia,  
Hang Tuah Jaya, 76100 Durian Tunggal, Melaka, Malaysia.  
Email: norfirdaus@utem.edu.my

---

## 1. INTRODUCTION

Generally, electrical generator is a device that converts mechanical energy obtained from an external source into electrical energy as an output. Permanent Magnet Generator is a generator that has many advantages such as high power coefficient and high efficiency. It can also operate at high speed applications. Various works have been carried out to analyse, model and characterize the performance of high power density generator. Some of them are determined for loss evaluation and design optimisation for direct driven PMG using simulation [1]. A few researchers intensively studied on the three-phase double stator permanent magnet generator that can produce higher power density and torque density. Nevertheless, most of them usually focus on the design optimisation of PMG for wind turbine application and for hybrid vehicles [2]-[9]. M. Norhisam et. al presents comparative evaluations on the power density of several types of double stator slot and slot-less topology of PMG that are purposely designed for agriculture sectors [10]. The power density evaluation is very important in order to design a portable PMG that is smaller, lightweight as well as high output power. In addition, double stator topology could maximize the usage of flux linkage which could increase power density [11]. A new structure for double stator brushless DC motor with thick pole shoe was proposed to improved energy [12]. However, the research only covered for single phase topology. In addition, many researchers study on five-phase machine modeling, but most of them are focusing on induction and synchronous machine [13]-[15]. None of them is conducting the study on the five-phase Double Stator Slotted Rotor Permanent Magnet Generator (DSSR-PMG). Most of them focused on the permanent magnet synchronous multiphase generators [16]-[18] that may have prospect for applications in

stand-alone self-excited generating systems in rural areas and low-power hydroelectric plants [19],[20]. In this paper, a five-phase DSSR-PMG is proposed for lower cogging torque and low voltage ripple compared to three-phase DSSR-PMG.

**2. BASIC STRUCTURE**

**2.1. Basic structure and configurations of DSSR-PMG**

Figure 1 shows the basic structure and equivalent magnetic circuit of the DSSR-PMG. It had been designed by employing a fractional numbers of slot per pole in order to reduce cogging torque. There are many ways others than employing a fractional numbers of slot per pole to reduce cogging torque such as skewing the stator or rotor slot, permanent magnet shaping and etc [21]. There are 18 slots 20 poles arrangement in three-phase configurations and 20 slots 18 poles in five-phase as shown in Figure 1 (a) and (b). Due to lower cogging torque, it is suitable for wind turbine application. Both models implement a slotted rotor whereas the permanent magnet (PM) are inserted between the rotor pole shoe with the advantage to prevent the PM's away from the initial position during operating at high speeds and does not require any glue to affix the magnets in the rotor. The equivalent magnetic circuit for both models is shown in Figure 1 (c) where  $\Lambda_{\delta_{os}}$  and  $\Lambda_{\delta_{is}}$  is the permeance for air gap and stator core in inner and outer stator,  $\Lambda_{m_{os}}$ ,  $\Lambda_{m_{is}}$  and  $F_{m_{os}}$ ,  $F_{m_{is}}$  are the PM permeance and magnetomotive force (MMF) in inner and outer stator,  $\Lambda_r$  and  $\Phi_m$  are the rotor permeance and PM flux,  $\Phi_{\delta_{os}}$ ,  $\Phi_{\delta_{is}}$  and  $\Phi_{\sigma_{os}}$ ,  $\Phi_{\sigma_{is}}$  are the main magnetic flux and leakage flux in the inner and outer stator, and  $F_{a_{os}}$ ,  $F_{a_{is}}$  is the stator armature (MMF) in inner and outer stator.

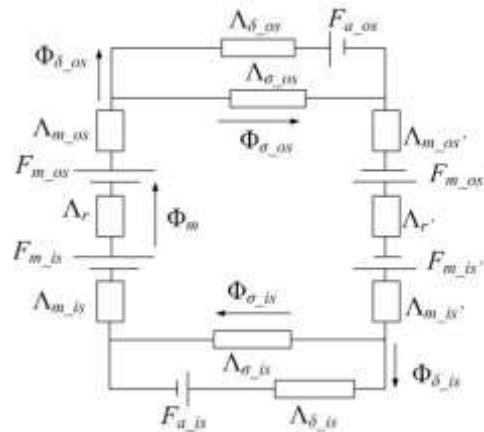
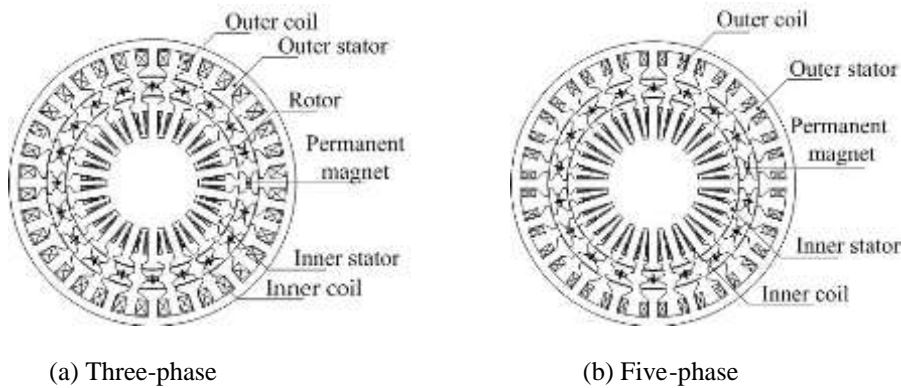


Figure 1. Basic structure and magnetic equivalent circuit of DSSR-PMG in this research

The proposed design consists of outer stator, inner stator, rotor, permanent magnet, outer and inner coil. The stators and rotor are made from non-oriented silicon steel (M250-35A) and Neodymium Boron Iron

(NdFeB 42) for permanent magnet. The coil is made from copper with 0.6 mm diameter by employing non-overlapping concentrated winding with double layer winding arrangement. The double layer winding are implemented for both design in order to limit the losses and torque ripple. Another advantages of using double layer configurations are shorter the end-windings, the lower harmonic content of MMF and reduced the eddy current losses in the permanent magnet [22]. The material used for five-phase DSSR-PMG are similar with three-phase design. The design parameters for both three and five-phase DSSR-PMG are listed in Table 1.

Table 1. DSSR-PMG specification

Parameters	DSSR-PMG	
	3-phase	5-phase
Outer stator diameter (mm)	156	156
Inner stator diameter (mm)	86	94
Number of slots	18	20
Number of poles	20	18
Number of phase	3	5
PM volume (m <sup>3</sup> )	$6.3 \times 10^{-7}$	$7.035 \times 10^{-7}$
PM size (mm)	$6 \times 2 \times 52.5$	$6.7 \times 2 \times 52.5$
Coil size (mm)	0.6	0.6
Stack length (mm)	52.5	52.5
Outer air gap (mm)	0.5	0.5
Inner air gap (mm)	0.5	0.5
No. of turns of inner coil	55	55
No. of turns of outer coil	55	55
Stator tooth face angle (°)	15	13
Stator tooth thickness (mm)	2	2
Stator tooth width (mm)	5	5
Outer stator slot opening (mm)	18.3	16.5
Inner stator slot opening (mm)	8.9	8.5
Outer stator tooth height (mm)	12	9
Inner stator tooth height (mm)	15	18

## 2.2. Phase and coil arrangements

The voltage generation process in PMG begins with the permanent magnets on the rotor produce a rotating magnetic field when it is turned by prime mover and thus induces the voltages within the stator windings. The winding layout and winding factor of the PMG depends on the combination of stator slot and poles. A phasor diagram in Figure 2 show the phase vector in mechanical displacement, whereas  $360^\circ/3 = 120^\circ$  for three-phase and  $360^\circ/5 = 72^\circ$  in five-phase.

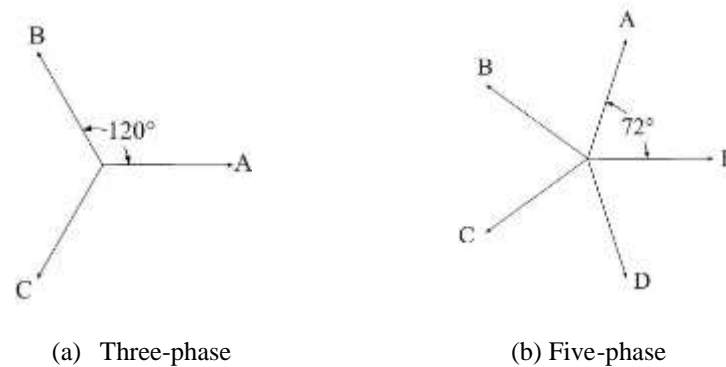


Figure 2. Phase vectors in mechanical degree

In this paper, the star of slots method is used to find the winding layout for both three and five-phase DSSR-PMG. For three-phase 18-slot/20-pole DSSR-PMG, each phase consists of six coils that are connected in series. While in five phase 20-slot/ 18-pole configurations, each phase has four coils that also connected in series. Both configurations are implementing of non-overlapping concentrated winding in series for both inner and outer stator with double layer winding arrangement to limit the losses and torque ripple. In order to achieve high fundamental winding factor, the number of slot per phase,  $q$  of DSSR-PMG is must lower than 0.5 but higher than 0.25. The number of slot per pole per phase is calculated as:

$$q = \frac{Q_s}{3P} \tag{1}$$

Where  $Q_s$  is the number of slots and  $p$  is number of poles. In this paper, the number of slot per pole per phase for three and five-phase DSSR-PMG are 0.3 and 0.37 respectively. Figure 3 (a) and (b) show mmf vector for each coils and coil winding arrangement for three and five phase DSSR-PMG whereas  $S$  means slot number inside the PMG. The coil vector arrangement for both structure are define by the electrical degree of the emf induced in the coil side of each slot. The angle between the phasor of two consecutive slot as per below:

$$Elec. degree = \frac{360}{Q_s} \times P_p \tag{2}$$

Where,  $P_p$  is number of pole pairs,  $Q_s$  is the number of slots. In this design,  $360/Q_s$  are refer to mechanical degree of the PMG. The mechanical and electrical degree are  $20^\circ$  and  $200^\circ$  for three-phase and  $18^\circ$  and  $162^\circ$  for five-phase configurations respectively.

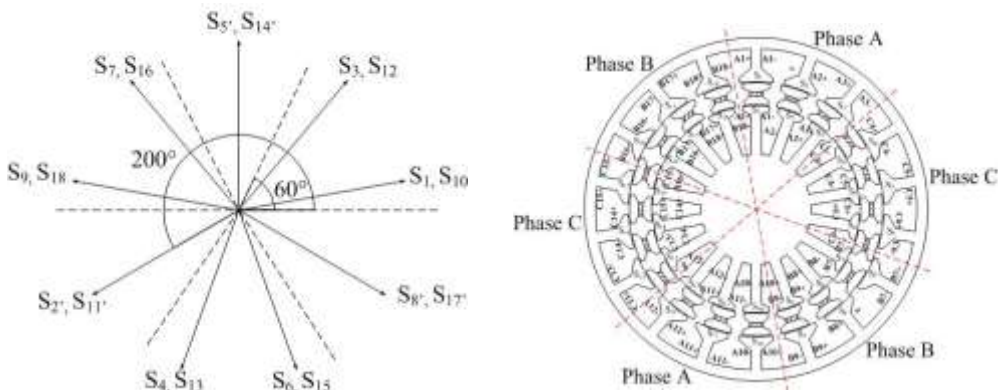
In order to allocate the winding arrangement in phase for each three (A, B, C) and five phase (A,B,C, D, E) DSSR-PMG, the sector of phase winding,  $W_s$  is determined as per below :

$$W_s = \frac{\pi}{n} \tag{3}$$

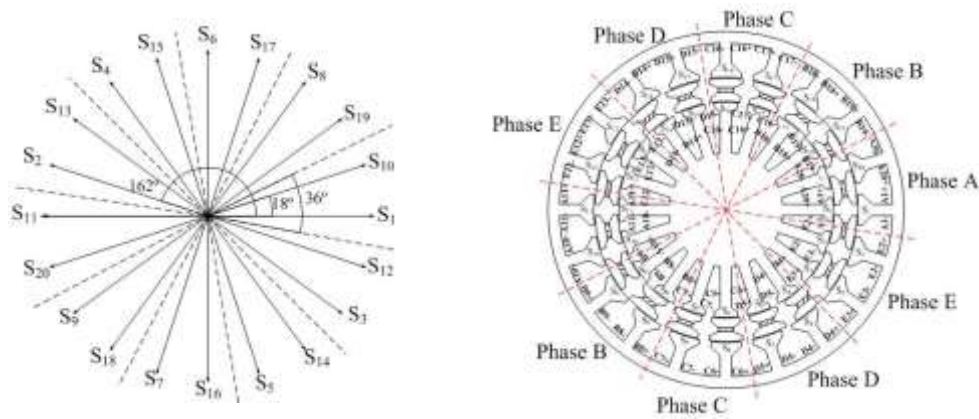
Where  $W_s$  is sector of phase winding in degree  $[\circ]$ ,  $n$  is the number of phases. In this paper, the  $W_s$  for three and five phase DSSR-PMG are  $60^\circ$  and  $36^\circ$  respectively. As can be seen from the Figure 3 (a), coil vectors and winding arrangement in three-phase DSSR-PMG, the phasor inside in the same sector are belonging same phase. It shown that for phase A, the vector numbers with  $S_1, S_2', S_3, S_{10}, S_{11}', S_{12}$  are in one sector in phase A. Since  $S_2'$  and  $S_{11}'$  are in opposite direction, it will be marked with apostrophe which means the coil in negative polarity which the same process are apply to phase B ( $S_7, S_8', S_9, S_{16}, S_{17}', S_{18}$ ) and C ( $S_4, S_5', S_6, S_{13}, S_{14}', S_{15}$ ), respectively. In three-phase DSSR-PMG, each phase contain of six slots whereas four slots in positive and the others two in negative polarity. From Figure 3 (b), in five-phase DSSR-PMG coil winding arrangement, the same method applied where it can be seen that the vectors numbered with  $S_1, S_{10}, S_{11}', S_{20}'$  are belonging to phase A. Similar for phase B, C, D, and E, which is contains four slots per phase with two slot in positive and two in negative polarity. The positive and negative polarity of the coil in the slots means the connections between each slots must be in series and sequence polarity in order to get a reliable and acceptable from the FEM. The complete coil vectors and winding arrangement for three and five-phase DSSR-PMG are listed in Table 2.

Table 2. DSSR-PMG phase and coil arrangements.

Phase	Coil arrangements	
	3-phase	5-phase
A	$S_1, S_2', S_3, S_{10}, S_{11}', S_{12}$	$S_1, S_{10}, S_{11}', S_{20}'$
B	$S_7, S_8', S_9, S_{16}, S_{17}', S_{18}$	$S_8, S_9', S_{18}', S_{19}$
C	$S_4, S_5', S_6, S_{13}, S_{14}', S_{15}$	$S_6, S_7', S_{16}', S_{17}$
D	-	$S_4, S_5', S_{14}', S_{15}$
E	-	$S_2, S_3', S_{12}', S_{13}$



(a) Three-phase DSSR-PMG



(b) Five-phase DSSR-PMG

Figure 3. Coil vectors and winding arrangement of three and five-phase DSSR-PMG

### 2.3. Back EMF and Flux linkage

The back-EMF is equal to the derivative with the time of the flux linkage created in the permanent magnet. In three and five-phase DSSR-PMG, there is dual flux linkage generated which is in inner and outer stator air gap. The correlation between flux linkage and back emf in PM machine as per equation below:

$$Emf = N \frac{d\phi}{dt} \quad (4)$$

where  $N$  is the number of turns,  $\phi$  is the rate of change of magnetix flux and  $t$  is the rate of change of time.

### 2.4. Cogging torque

The cogging torque is generated by the variation of the magnetic permeance by the PM due to the slotting of the stator surface, even when there is no stator excitation [23]. In theoretically, the cogging torque,  $T_{cog}$  of permanent magnet machine is determine as per below:

$$T_{cog} = -\frac{1}{2} \phi_g^2 \frac{d\mathfrak{R}}{d\theta} \quad (5)$$

where  $\phi_g^2$  is the flux in the air gap,  $\mathfrak{R}$  is the reluctance in the air gap and  $\theta$  is the degree of the rotor position [24]. Cogging torque waveform for both models was simulated by 2D FEA (Ansys Maxwell) with the using of desktop computer with the processor of Intel i7-4790 CPU 3.6 GHz with RAM memory of 12 GB. The computation process will take approximately 15 minutes to solve a model at one desired speed.

## 3. PERFORMANCE COMPARISON

In order to have a fair comparison, both models have been modeled with similar size and volume of rotor, stator and permanent magnet. The total number of turns and the total length of inner and outer airgap are similar for both models. The simulation results of flux linkage and no-load electromotive force (EMF) are conducted by using 2D FEM on three and five-phase models. Figure 4 (a) and (b) shows the flux linkage for both inner and outer stator and no-load EMF waveforms for three-phase and five-phase DSSR-PMG at rated speed of 2000 rpm. It can be seen that the maximum value of three-phase is around 0.15 Wb whereas for five-phase DSSR-PMG is 0.12 Wb. The three-phase DSSR-PMG has 20% higher than five-phase DSSR-PMG. It shown that five-phase DSSR-PMG has a lower flux linkage compared to-three phase DSSR-PMG. The lower value of flux linkage in five-phase DSSR-PMG is because the total number of turns per slot per phase is less than three-phase which are 440 turns and 660 turns for both in inner and outer stator. Taking into account the low value of flux linkage in five-phase DSSR-PMG, it will also affect the output of the back EMF.

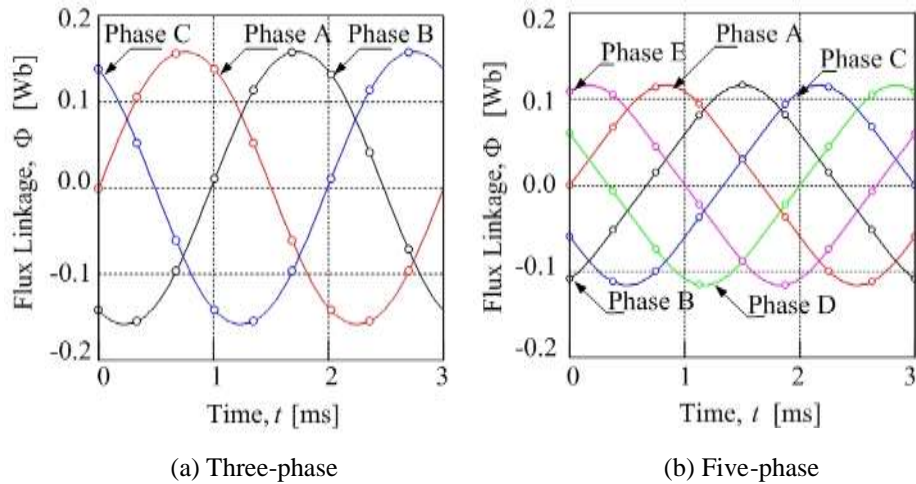


Figure 4. Flux linkage at rated speed 2000rpm

Figure 5 (a) and (b) show the waveforms of no-load EMF three-phase and five-phase DSSR-PMG. The waveform in three-phase DSSR-PMG are more sinusoidal compared to five-phase is more close to trapezoidal one. It can be observed that the phase voltage amplitude has been reduced and waveforms of no-load EMF for both three and five-phase DSSR-PMG are symmetrical. It can be deduced from the waveforms that the peak value of three-phase DSSR-PMG is 343 V whereas for five-phase is 180 V. As can be seen from the waveforms, the amplitude for five-phase DSSR-PMG is lower than three-phase DSSR-PMG. It is recorded a 52% decrease in value of the no-load EMF for five-phase DSSR-PMG compared to three-phase DSSR-PMG. When it converted to DC, the ripple voltage of back-EMF in five-phase DSSR-PMG is significantly lower than three-phase. The ripple percentage in a three-phase is 55% whereas for five-phase DSSR-PMG is been reduced to 2.3%.

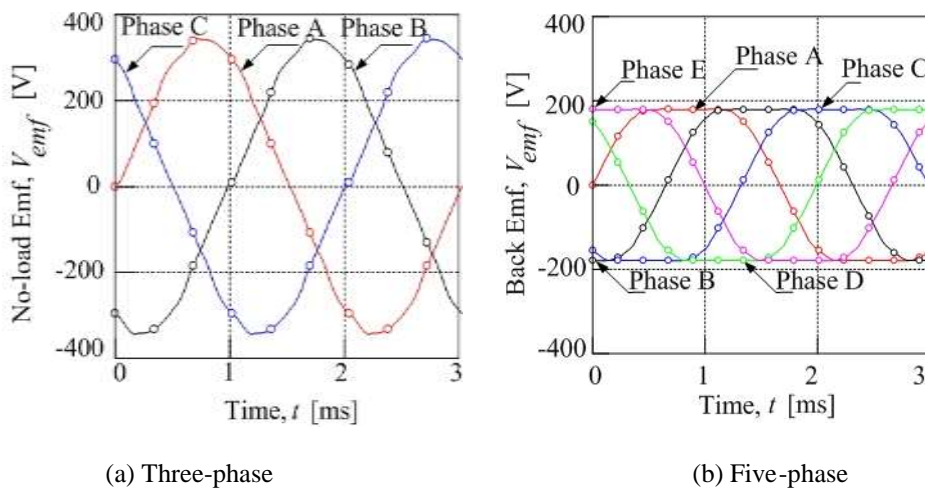


Figure 5. No-load EMF at rated speed 2000rpm

The back-EMF and cogging torque value are simulated in FEM at no-load condition as shown in Figure 6. The cogging torque produced by the interaction of poles and stator slot opening when the stator in open circuit. Figure 6 (a) show the cogging torque (peak to peak value) of three and five-phase DSSR-PMG at rated speed of 2000 rpm. It can be observed that, the five-phase cogging torque is reduced about 80% compared to the three-phase. The maximum value of cogging torque for three and five-phase DSSR-PMG is 0.35Nm and 0.07Nm, respectively. It can be concluded that the cogging torque in five-phase DSSR-PMG is effectively reduced due to fact that in five-phase systems, each electrical revolution generates 10 pulses per

cycle while in three-phase is 6 pulse for each cycle in order to deliver the same energy. Thus three-phase DSSR-PMG need to have larger magnitude pulses. Figure 6 (b) shows that the back-EMF in rms value for both three-phase and five-phase DSSR-PMG. It can be seen that the back-EMF is increasing as the speed increases in proportionally linear to the speed. The maximum value of three-phase DSSR-PMG is 310 V whereas for five-phase is around 240 V. It can be deduced from the graph that the back-EMF for five-phase DSSR-PMG is lower than three-phase DSSR-PMG as the speed increases. This is due to flux linkage which affects the output of back-EMF of five-phase DSSR-PMG. The analysis of simulations results for three and five-phase DSSR-PMG as per tabulated in Table 3.

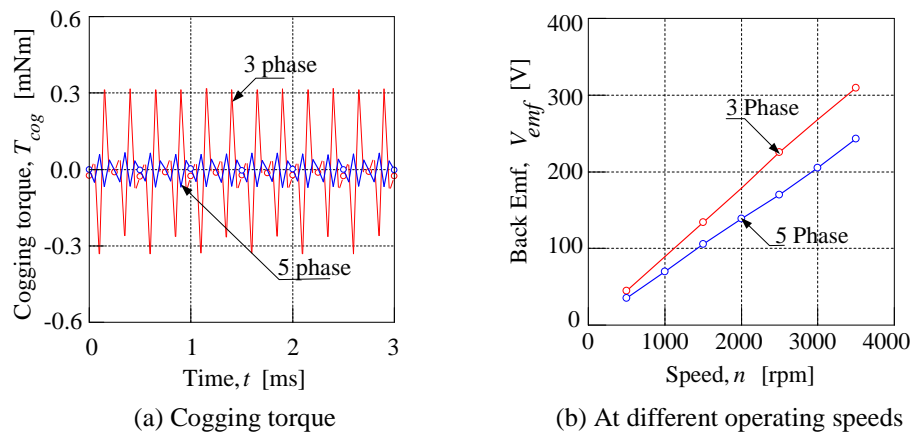


Figure 6. Back-EMF and cogging torque of 3 and 5-phase DSSR-PMG

Table 3. Analysis results of three and five-phase DSSR-PMG using FEM

Parameters	Unit	DSSR-PMG	
		Three-phase	Five-phase
Max. per phase Flux linkage	Wb	0.15	0.12
Max. per phase Back-EMF, $V_{emf}$	$V_{rms}$	343	180
Cogging torque, $T_{cog}$	$N_m$	0.35	0.07
Percentage of voltage ripple, $V_{ripple}$	%	55	2.3

#### 4. CONCLUSION

As conclusion, the models of three-phase and five-phase DSSRPMG have been simulated and developed. This model developed with the implementation of double stator structure for both three and five-phase models. The simulation results show the ripple voltage (peak to peak) of back-EMF in five-phase is 2.3% compared to the three-phase DSSR-PMG which is 55%. It can be observed that, the five-phase cogging torque is 80% reduced compared to the three-phase DSSR-PMG. The proposed model of five-phase DSSR-PMG is suitable to use in wind power generations and stand-alone generator to generate electricity in rural areas. The design model of three and five-phase DSSR-PMG will be fabricated in future in order to verified the simulation and experimental results. In addition, a performance characteristic comparison for both model will be done.

#### ACKNOWLEDGEMENTS

The authors would like to thank Ministry of Education, Universiti Teknikal Malaysia Melaka (UTeM) and Universiti Putra Malaysia for providing the research grant FRGS/1/2014/TK03/FKE/02/F00208 and FRGS/1/2015/TK04/FKE/02/F00260, PJP/2015/FKE(5A)/S01478, PJP/2016/FKE(H15)/S01478, and RACE/F3/TK14/FKE/F00250, for this research.

#### REFERENCES

- [1] S. Eriksson, *et al.*, "Loss evaluation and design optimisation for direct driven permanent magnet synchronous generators for wind power," *Applied Energy*, pp. 265-271, 2011.
- [2] H. W. Kim, *et al.*, "Modeling and control of PMSG-based variable-speed wind turbine," *Applied Energy*, vol. 80, pp. 46-52, 2010.

- [3] D. G. Dorrell, "Design Requirements for Brushless PM Generator for used in Small Renewable Energy Systems," The Annual Conference of IEEE Industrial Electronics Society (IECON), pp. 216-221, 2007.
- [4] X. Liu, *et al.*, "A Novel Dual-Stator Hybrid Excited Synchronous Wind Generator," *IEEE Transactions on Industry Applications*, vol/issue: 45(3), pp. 947-953, 2009.
- [5] Y. Li, *et al.*, "A Novel Direct Torque Control Permanent Magnet Synchronous Motor Drive used in Electrical Vehicle," *International Journal of Power Electronics and Drive Systems (IJPEDS)*, vol/issue: 1(2), pp. 129-138, 2011.
- [6] S. Niu, *et al.*, "A Permanent-magnet Double-stator Integrated starter-generator for Hybrid Electric Vehicles," IEEE Vehicle Power and Propulsion Conference (VPPC), pp. 1-5, 2008.
- [7] D. Zhang, *et al.*, "Design and Analysis of a Double-Stator Cup-Rotor Directly Driven Permanent Magnet Wind Power Generator," Power Electronics and Motion Control Conference, vol. 3, pp. 1-5, 2006.
- [8] I. Tarimer, "Designing an Efficient Permanent Magnet Generator for Outdoor Utilities," *International Journal of Engineering Science and Innovative Technology (IJESIT)*, vol/issue: 3(3), pp. 543-548, 2014.
- [9] Y. H. Chen, *et al.*, "PM Wind Generator Topologies," *IEEE Transactions on Industry Applications*, vol. 41, pp. 1619-1626, 2005.
- [10] M. Norhisam, *et al.*, "Comparative Evaluation on Power-Speed Density of Portable Permanent Magnet Generator For Agriculture Applications," *Progress in Electromagnetics Research*, vol. 129, pp. 345-363, 2012.
- [11] M. Norhisam, *et al.*, "Comparison on Performance of a Single Phase and Three Phase Double Stator Type Permanent Magnet Generator," *Asia-Pacific Symposium on Applied Electromagnetics and Mechanics, Kuala Lumpur*, pp. 231-34, 2010.
- [12] N. F. Raja, *et al.*, "Improvement of Energy Density in Single Stator Interior Permanent Magnet Using Double Stator Topology," *Mathematical Problems in Engineering*, pp. 1-15, 2014.
- [13] L. A. Pereira, *et al.*, "Model of a five-phase induction machine allowing for harmonics in the air-gap field, Part I: Parameter determination and general equations," in Proc. IEEE IECON, pp. 98-103, 2004.
- [14] R. Ilka, *et al.*, "Optimum Design of a Five Phase Permanent Magnet Synchronous Motor for Underwater Vehicles by use of Particle Swarm Optimization," *TELKOMNIKA Indonesian Journal of Electrical Engineering*, vol/issue: 10(5), pp. 925-932, 2012.
- [15] L. Parsa, *et al.*, "Five-phase interior permanent-magnet motors with low torque pulsation," *IEEE Trans. Ind. Appl.*, vol/issue: 43(1), pp. 40-46, 2007.
- [16] D. Vizireanu, *et al.*, "Investigation on multi-star structures for large power direct-drive wind generator," *Electr. Power Compon. Syst.*, vol/issue: 35(2), pp. 135-152, 2007.
- [17] D. Vizireanu, *et al.*, "Design and optimization of a 9-phase axial-flux PM synchronous generator with concentrated winding for direct-drive wind turbine," in Conf. Rec. IEEE IAS Annu. Meeting, Tampa, FL, pp. 1912-1918, 2006.
- [18] G. K. Singh, *et al.*, "Analysis of a saturated multiphase (six-phase) self-excited induction generator," *Int. J. Emerging Electr. Power Syst.*, vol/issue: 7(2), pp. 1-21, 2006.
- [19] S. Kato, *et al.*, "A low-cost system of variable-speed cascaded induction generators for small-scale hydroelectricity," in Conf. Rec. IEEE IAS Annu. Meeting, Chicago, IL, pp. 1419-1424, 2001.
- [20] G. K. Singh, *et al.*, "Analysis of a saturated multiphase (six-phase) self-excited induction generator," *Int. J. Emerging Electr. Power Syst.*, vol/issue: 7(2), pp. 1-21, 2006.
- [21] S. Paulsamy, "Reduction of Cogging Torque in Dual Rotor Permanent Magnet Generator for Direct Coupled Wind Energy Systems".
- [22] O. Barré, *et al.*, "Concentrated Windings in Compact Permanent Magnet Synchronous Generators: Managing Efficiency," *Machines*, vol/issue: 4(2), pp. 1-32, 2016.
- [23] F. Mier, "Permanent Magnet Synchronous Machines with Non-Overlapping Concentrated Windings for Low-Speed Direct-Drive Applications," PhD thesis, Royal Institute of Technology, 2008.
- [24] D. Hanselman, "Brushless Permanent-Magnet Motor Design," New York, McGraw-Hill, 1994.

## BIOGRAPHIES OF AUTHORS



**R. Suhairi** was born on 13 June 1984 at Kota Bharu Kelantan. He received the B. Eng. in Industrial Electronics from Universiti Malaysia Perlis, Malaysia in 2009, and M. Sc. in Electrical Power Engineering from Universiti Putra Malaysia, Malaysia in 2012. Currently he is pursuing his Ph. D. in electrical machine design at Universiti Teknikal Malaysia Melaka. His research interests are electrical machine design, electric machine simulation, electric drives, and energy conversion.



**R. N. Firdaus** was born on May 1982 at Parit Buntar, Perak, Malaysia. He received B. Eng., M.Sc. and Ph.D. in Electrical Power Engineering from Universiti Putra Malaysia. In 2006, 2009 and 2013, respectively. He is currently senior lecturer in Department of Power Electronics and Drives, Faculty of Electrical Engineering, Universiti Teknikal Malaysia Melaka. His research interest includes applied magnetics, electrical machines, magnetic sensor and drives.



**F. Azhar** is a senior lecturer at the Faculty of Electrical Engineering, Universiti Teknikal Melaka, Malaysia (UTeM), Melaka. He has been with UTeM since 2005. He received his B. Eng. Degree in Electrical and Electronic Engineering and M.Sc. of Electrical Engineering from Universiti Putra Malaysia in 2002 and 2009 respectively. On 2009, he received his Ph. D Eng in Machine Design from Shinshu University, Japan. His areas of interest include electrical machine and actuator design, numerical analysis and machine drive.



**K. A. Karim** received the M.Sc. from University of Bradford and Ph. D. degrees from the University of Nottingham, UK, in 2003 and 2011, respectively. He is currently a Senior Lecturer with the Department of Power Electronics and Drives, Faculty of Electrical Engineering, Universiti Teknikal Malaysia Melaka, Durian Tunggal, Malaysia. His research interests include electrical machine design, power electronics, and electric vehicle.



**A. Khamis** is a senior lecturer at the Faculty of Electrical Engineering, Universiti Teknikal Melaka, Malaysia (UTeM), Melaka. She received her B. Eng. Degree in Electrical & Electronics Engineering (Electrical Power) from Universiti Putra Malaysia in 2006. On 2008, she received her M.Sc. Power Distribution from Newcastle University, United Kingdom. On 2014 and 2016, she receive her Ph.D Eng and Post Doctoral respectively from Universiti Kebangsaan Malaysia and The University of Sydney Australia.